Lattice dynamics, structural stability, and phase transitions in incommensurate and commensurate A_2BX_4 materials

I. Etxebarria, J. M. Perez-Mato, and G. Madariaga
Departamento de Física de la Materia Condensada, Facultad de Ciencias, Universidad del Pais Vasco, Apartado 644, Bilbao, Spain
(Received 10 December 1991)

Numerous materials with the general formula A_2BX_4, where A and B are cations and X is the anion, are isomorphous to β-K_2SO_4 (space group *Pnam*) at high temperatures. A considerable number of them exhibit a structural instability leading to an incommensurately modulated phase with identical superspace symmetry. K_2SeO_4 is the archetypical example. From the analysis of the incommensurate structures, the polarization vector of the unstable frozen mode can be determined, being similar in all investigated compounds. We report here a comparative energetic study and lattice-dynamics analysis of a set of compounds in this family. The set of materials K_2SO_4, Rb_2SeO_4, Cs_2SeO_4, Cs_2ZnCl_4, Cs_2ZnBr_4, K_2CrO_4, K_2SeO_4, K_2ZnCl_4, Rb_2ZnCl_4, and Rb_2ZnBr_4, includes compounds with and without an incommensurate phase. An empirical rigid-ion force model has been used with only three adjustable parameters, the tetrahedral BX_4 groups being reduced to rigid bodies. The adjusted force model, optimized for each compound with use of only static structural data, is sufficient to explain the eventual presence of an incommensurate lattice instability at lower temperatures. The calculated phonon dispersion curves of those compounds with an incommensurate phase include an unstable Σ_2 phonon branch with a minimum close to $\frac{1}{3}\mathbf{a}^*$. In the simulations, the unstable or soft-mode branch is always an optical branch in the extended zone scheme or the consequence of an anticrossing of an optical branch with the Σ_3-Σ_2 acoustic branch; this result discredits any attempt to explain the soft-mode mechanism in terms of a one-dimensional model with an acoustic soft branch. The polarization vectors of the soft or unstable modes obtained in the simulations fairly agree with the experimental ones. They are rather insensitive to the details of the interactions, explaining their strong similarities. On the other hand, the form of the soft branch depends strongly on the material, and clearly distinguishes those materials having the BX_4 groups disordered in the normal phase, from those having a soft-mode mechanism. The simulations indicate that the static and dynamic features of potassium chromate are similar to those of potassium selenate, raising the possibility that potassium chromate could exhibit a similar mode softening at low temperatures. The existence of an incommensurate lattice instability in these compounds depends basically on the effective volume of the A cations compared with the size of the BX_4 tetrahedra. The charge distribution within the tetrahedral anion groups also plays a significant secondary role; smaller values of the charge of B tend to stabilize the *Pnam* structure. The static energy of some of the compounds has been investigated in a restricted configuration subspace, which includes the order-parameter distortion. The energy maps obtained show a clear "multiple-well" structure, that can be quantitatively related with the transition temperatures by means of a local-mode model.

I. INTRODUCTION

Many materials of the type A_2BX_4, isomorphous with β-K_2SO_4 (space group *Pnam*), transform at lower temperatures into an incommensurately modulated (IC) phase with the modulation wave vector along the a axis. In most cases the modulation wave vector is close to the value $\frac{1}{3}\mathbf{a}^*$. The symmetry of the distorting mode (order parameter) is Σ_2 (antisymmetric for the a and m symmetry planes). If the temperature is further decreased, a second phase transition into a commensurate phase takes place and the modulation wave vector locks into a commensurate value, which is $\frac{1}{3}\mathbf{a}^*$ in many materials. This general scheme is reproduced in most of the compounds, but particular features vary considerably. The compounds of Zn (Rb_2ZnCl_4, Rb_2ZnBr_4, and K_2ZnCl_4) do not exhibit a proper soft-phonon branch, and the tetrahedral groups BX_4 seem to be disordered in two equivalent positions in the *Pnam* normal phase.[1] In contrast, a clear Σ_2 soft mode has been observed in K_2SeO_4,[2] and for this compound x-ray structural analyses of the normal phase have been successful using nondisordered models.[3,4] For a general review see Refs. 5 and 6.

The incommensurate instability observed in these compounds has an essentially common origin. This is shown, for instance, by the similarity of the polarization vectors describing the primary distorting mode in the IC phase. The static displacement of each atom or atomic group with respect to its position in the average commensurate structure is given in the sinusoidal regime by

$$\mathbf{u}(\mu,l)=\tfrac{1}{2}\{Q\mathbf{e}(\mu)\exp[i\mathbf{q}\cdot(l+\mathbf{r}_\mu)]+\text{c.c.}\}\ , \qquad (1)$$

where (μ,l) labels the atom at $l+\mathbf{r}_\mu$ in the average structure, l being the lattice vectors of the average structure, while $\mathbf{q}$ is the modulation wave vector and Q is a global complex amplitude, with arbitrary phase if $\mathbf{q}$ is incom-

mensurate. The actual structure of the modulation is then essentially given by the complex polarization vector or "eigenvector" $\mathbf{e}(\mu)$. The complex normal coordinate Q can be identified with the order parameter of the normal-IC phase transition. In accordance with this description, it is normally observed that the modulation polarization vector $\mathbf{e}(\mu)$ is approximately constant as the temperature is lowered, the temperature variation of the modulation being restricted to the order parameter Q and the modulation wave vector $\mathbf{q}$. A comparison of the experimental value of the polarization vector $\mathbf{e}(\mu)$ in a series of A_2BX_4 compounds[7,8] with IC phases showed striking similarities among the different structural modulations, specially with respect to the relative phase shifts of the different structural modulations. Only in the case of potassium selenate, some significant differences with respect to the other materials can be observed, especially in the ratio of the amplitudes of the rotations around the a and b axes.[7] Hence, the structure of the IC modulation is not very sensitive to the details of interatomic interactions and seems to depend essentially on some of the common static features of these materials.

The microscopic mechanism of the incommensurate structural instability in these compounds has been investigated by studying the lattice dynamics of rigid-ion models.[9–13] These models were quite successful in reproducing the essential features of the observed behavior, and were mostly based on "*ab initio*" interatomic potentials. Recently, we have performed an analysis of the lattice dynamics of K_2SeO_4 within an empirical rigid-ion model.[7] The model was extremely simplified, with two to five adjustable parameters, the BX_4 anions being reduced to rigid bodies. The models parameters were adjusted using a systematic minimization procedure of the differences between the calculated equilibrium atomic configuration (restricted to *Pnam* symmetry) and the experimental *Pnam* normal structure. The results of this work indicated that an empirical rigid-ion force model consistent with the static structural data was enough to reproduce the basic features of the incommensurate structural instability, predicting an unstable soft mode with the characteristics observed experimentally. The effective size of the potassium atoms in comparison with the size of the selenate tetrahedra and some particular interacting K-O pairs played a fundamental role in the mode softening mechanism.

The success of the simulation in potassium selenate suggested that a similar procedure could be applied to a whole set of A_2BX_4 materials (with and without IC phases). A comparative study along similar lines for a significant number of compounds can clarify the conditions leading to the eventual existence of an IC phase, and the predictive power of the method in accounting for the differences and similarities between the materials. We report here the results of a study of this type. The set of compounds investigated are K_2SO_4, Rb_2SeO_4, Cs_2SeO_4, Cs_2ZnCl_4 Cs_2ZnBr_4, K_2CrO_4, K_2SeO_4, K_2ZnCl_4, Rb_2ZnCl_4, and Rb_2ZnBr_4. For the first six ones there is no contrasted evidence of any instability of the *Pnam* phase up to very low temperatures, while the last four exhibit the mentioned normal-IC phase transition at 130 K, 553 K, 303 K, and 347 K, respectively.[6] For each of these compounds, the knowledge of the static structure at the *Pnam* phase has been used to optimize a rigid-ion force model with only three adjustable parameters. The lattice dynamics corresponding to the optimized model has been investigated. In particular, the phonon branches along the $\mathbf{a}^*$ direction have been calculated. The results for the different materials can be related in a direct and simple manner with their structural thermal properties and the eventual presence of an incommensurate structural instability.

In order to obtain more quantitative predictions, the double-well structure of the configurational energy of some of the compounds has been investigated in a restricted subspace related with the order parameter of the tripled ferroelectric phase. Then, a local-mode approximation can be introduced. The energetics of the materials can be parametrized in terms of an effective Hamiltonian representing a chain of coupled double wells. An estimation of the transition temperatures can then be derived, which agrees fairly well with the available experimental data. Part of the present work was presented in a preliminary form in Ref. 14.

The contents of the paper are as follows: in Sec. II, the characteristics of the force model used and its adjustment procedure for each compound are discussed. The lattice-dynamics calculations are presented in Sec. III. In Sec. IV the energetics of the different systems is investigated within the subspace of distortions associated to the order parameter of the commensurate lock-in phase. The parametrization of the energetics of the materials in terms of an effective local-mode Hamiltonian is discussed in Sec. V. Section VI is finally devoted to some concluding remarks.

II. INTERATOMIC FORCE MODEL

As interatomic interactions, only point-charge Coulombic and short-range repulsive Born-Mayer forces are considered. The point charge of A cations has been taken as $+1e$, the net charge in the BX_4 groups being restricted to $-2e$. Following Chaplot and Rao,[15,16] the Born-Mayer potentials were introduced in the form

$$V_{\text{rep}}(r_{ij}) = A \exp(-br_{ij}/[R_i + R_j]) , \tag{2}$$

where $A = 1822$ eV and $b = 12.364$ Å^{-1} are common for all atoms, the parameters R_i being some effective radius associated to each atom type. Repulsive forces between B atoms and atoms out of the BX_4 anions can be neglected. The tetrahedra BX_4 are considered rigid bodies, having the configuration observed at the *Pnam* phase. The adjustable model parameters are then limited to R_A, R_X, and the point charge of atom B, Q_B.

The optimization of the force model was done for each compound using the fitting procedure described in Ref. 7. The model parameters were adjusted so that they minimize a numerical factor measuring the structural differences, with respect to atomic positions and lattice parameters, between the calculated equilibrium configuration and the observed normal *Pnam* structure.

For some compounds, the results of structural analyses

of the normal phase situate the positions of the BX_4 groups split between two different configurations related by the mirror plane perpendicular to the c axis. In these cases, we have taken as "observed" configuration of the tetrahedra that obtained by closing together (perpendicularly to the mirror plane) the splitted configurations so that the central atom lies on the mirror plane and then rotating both configurations up to the disappearance of the splitting of the oxygen atoms.

The minimization process is done using a simplex algorithm,[17] while the "equilibrium" or "relaxed" structure for a given set of model parameters is calculated by means of the program WMIN.[18] For more details we refer the reader to Ref. 7. The calculation of the "equilibrium" configuration is done under the symmetry restrictions of space group *Pnam*. The stability of the calculated structure is therefore not guaranteed, and the configuration may be unstable with respect to symmetry-breaking distortions. However, in the cases we have studied, the condition is restrictive enough to obtain a unique set of energetic model parameters consistent with the basic features of the observed static structure. The eventual existence of unstable symmetry-breaking modes can then be related to intrinsic instabilities of the structure. These instabilities are susceptible of being thermally deactivated at high temperatures by anharmonic renormalization effects, explaining the existence of a structural phase transition at lower temperatures.

As the effect of the short-range repulsive interactions A-A on the calculated phonon branches was practically negligible in all cases, a second fitting process was done setting to zero this interaction. The values of R_X changed drastically with respect to the first adjustment, but R_A+R_X, which determines the repulsive A-X interaction, and the charge Q_B are essentially maintained. This second fitting is systematically better than the first one, indicating that the X-X interaction can be better simulated in this form. By neglecting the A-A repulsive forces of the form (2), the Born-Mayer A-X and X-X interactions become in fact uncorrelated and the X-X interaction is significantly reduced. In the following, the results presented refer to this second model that neglects A-A short-range repulsive interactions.

The structural experimental data necessary for the fitting of the force model of K_2SO_4, K_2CrO_4, K_2SeO_4, Rb_2SeO_4, Cs_2SeO_4, Cs_2ZnCl_4, Cs_2ZnBr_4, K_2ZnCl_4, Rb_2ZnCl_4, and Rb_2ZnBr_4 were taken from Refs. 19, 5, 20, 21, 22, 23, 24, 25, and 26, respectively. The optimized model parameters are shown in Table I. The F factor is the minimized parameter, defined in Ref. 7, measuring the difference of the calculated equilibrium structure with respect to the experimental one. Roughly, the value $F=1$ implies a mean deviation of 0.1 Å in atomic positions and 1% deviation in lattice parameters.[7]

The parameter R_T shown in Table I is the average value of the experimental B-X interatomic distances inside tetrahedra. The last column in this table lists the ratio $R_T/(R_A+R_X)$ obtained for each compound as a relative measure of the free space left to the BX_4 groups inside the crystal. It will be shown below that, for a given BX_4 group, this value—which decreases when increasing the size of the cation A—can be correlated with the IC phase transition temperature or the lack of a phase transition at all.

The charge distribution obtained for the BX_4^{2-} anions in the oxygen compounds is rather different from the one in the chlorine and bromine compounds, while having similar values within the two groups. Only potassium chromate seems to be an exceptional intermediate case. It is interesting to notice that the charge obtained for Se and S atoms (around $1.25e$) in the oxygen compounds is similar to the value $1.15e$ recently derived from quantum chemistry calculations[13] for the ion SeO_4^{2-}, but differs considerably from the result ($1.64e$) of a similar calculation[27] reported for SO_4^{2-}. It is also quite different from the one proposed ($2e$) in Refs. 9 and 19 for the groups SeO_4^{2-} and SO_4^{2-}, respectively. The charge values obtained for Zn (around $0.5e$) differ considerably from the hypothesis of fully ionized halogen atoms ($Q_{Zn}=+2e$) as

TABLE I. Fitted model parameters (R_A,R_X,Q_B) for each compound. F is the minimized parameter measuring the deviation of the experimental *Pnam* structure from that predicted by the force model. Some relevant quantities [R_A+R_X,RT,$RT/(R_A+R_X)$] involved in the stability of these compounds, as cited in the text, are also listed.

	R_A (Å)	R_X (Å)	Q_B (e)	F	R_A+R_X (Å)	RT (Å)	$RT/(R_A+R_X)$
K_2CrO_4	2.8754	0.7063	0.977	0.142	3.5817	1.6433	0.4588
K_2SO_4	2.8691	0.6999	1.272	0.092	3.5690	1.4691	0.4116
K_2SeO_4	2.8148	0.7924	1.215	0.156	3.6072	1.6260	0.4508
Rb_2SeO_4	3.0687	0.6754	1.177	0.147	3.7441	1.6404	0.4382
Cs_2SeO_4	3.1331	0.8176	1.330	0.109	3.9507	1.6366	0.4143
K_2ZnCl_4	3.1869	0.8726	0.733	0.067	4.0595	2.2217	0.5473
Rb_2ZnCl_4	3.5082	0.6538	0.518	0.063	4.1620	2.2425	0.5388
Cs_2ZnCl_4	3.8116	0.5327	0.309	0.195	4.3443	2.2589	0.5200
Rb_2ZnBr_4	3.5294	0.8155	0.484	0.105	4.3449	2.3772	0.5471
Cs_2ZnBr_4	3.6647	0.8480	0.282	0.212	4.5127	2.3874	0.5290

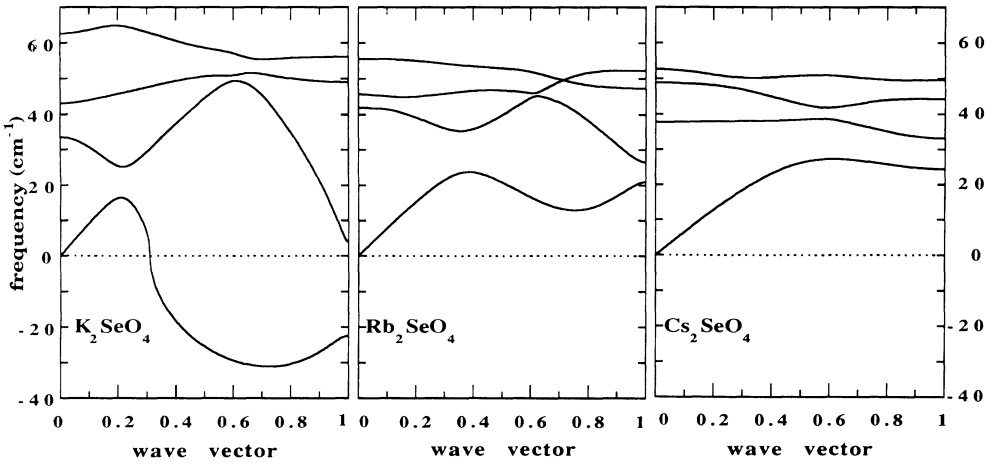

FIG. 1. Four lowest Σ_3-Σ_2 phonon branches for K_2SeO_4, Rb_2SeO_4, and Cs_2SeO_4 calculated according to the force models of Table I, and plotted in the extended zone scheme. In the case of "unstable" imaginary frequencies, their moduli with negative sign are represented.

considered in Refs. 10–12. They are closer to the value of 1*e* proposed in Refs. 22 and 28, and fairly agree with the value of 0.6*e* for Cu in Cs_2CuCl_4 proposed in Ref. 29.

III. LATTICE DYNAMICS

Phonon dispersion curves have been calculated for all the materials using the force models reported in the previous section and the program DYN described in Ref. 30. The BX_4 groups were taken as rigid units, and only external vibrational dispersion branches were considered.

The obtained four lowest Σ_3-Σ_2 phonon branches are shown in the extended zone scheme in Fig. 1 for the three selenium compounds. In the case of Cs_2SeO_4, the prolongation of the acoustic branch has its minimum at $\mathbf{q}=\mathbf{a}^*$, while in Rb_2SeO_4 a strong softening of the branch can be seen close to $0.7\mathbf{a}^*$. In K_2SeO_4, the lowest branch is unstable as obtained in Ref. 7, with imaginary frequencies for a significant range of wave vectors, while the minimum of the squared frequency is also close to $0.7\mathbf{a}^*$. This last result does not discredit the force model employed. On the contrary, it can be interpreted as a prediction of the observed low-temperature instability. Indeed, recent molecular-dynamics calculations[31] using the same force model have shown that thermal effects are sufficient to renormalize the mentioned unstable frequencies into real values and thermally stabilize the mechanically unstable branch of Fig. 1. The effective frequency values of the lowest Σ_3-Σ_2 branch obtained in the molecular-dynamics simulation at 250 K are not only real, but in fair agreement with the experimental ones.[31]

Both in the cases of Rb_2SeO_4 and K_2SeO_4, the conspicuous softening of the lowest Σ_2 branch is the result of the "anticrossing" of the acoustic branch with an optic one, the unstable or soft branch being essentially the prolongation of the lowest Σ_3-Σ_2 optic branch.

The form of the lowest Σ_3-Σ_2 branch for Rb_2SeO_4 is similar to the experimental one for K_2SeO_4 at temperatures above the normal-IC phase transition. This suggests that the thermal effect on the form of the phonon branch can be attributed in a qualitative form to an increase of the effective size of the *A* cations as a result of the thermal vibrations. The critical role played by the effective size of the *A* ions and the resulting repulsive *A*-*X* interaction on the Σ_2 branch softening can be seen in Fig. 2, where the changes in the calculated lowest-energy branch of Rb_2SeO_4 are shown as the Rb effective radius is increased and decreased in an amount of 0.5%. It would be interesting to check experimentally if this compound, for which there is no evidence of a phase transition at low temperatures, exhibits at least a partial softening of the branch, as suggested by these results.

The calculated lowest Σ_3-Σ_2 branches corresponding to K_2SO_4 and K_2CrO_4 are shown in Fig. 3. Again, the anticrossing between the acoustic branch and the first optical one is a basic feature. Comparing with Fig. 1, K_2SO_4 can be considered from the dynamical point of view an intermediate case between Rb_2SeO_4 and Cs_2SeO_4. The smaller size of the tetrahedral anions SO_4^{2-} (see Table I)

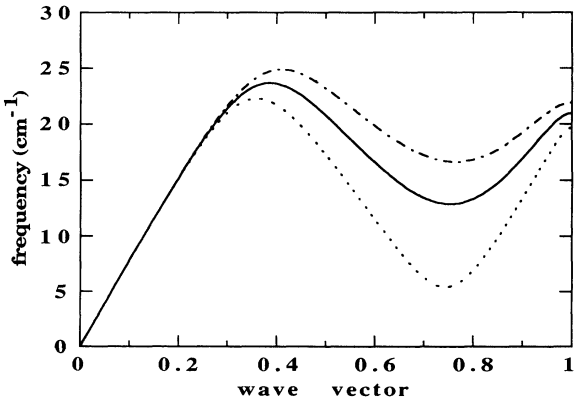

FIG. 2. Lowest Σ_3-Σ_2 phonon branch in the extended zone scheme of Rb_2SeO_4 calculated according to the corresponding force model in Table I (solid line), and also for stronger (dashed line) and weaker (point line) Rb-O interactions by an amount of 0.5%.

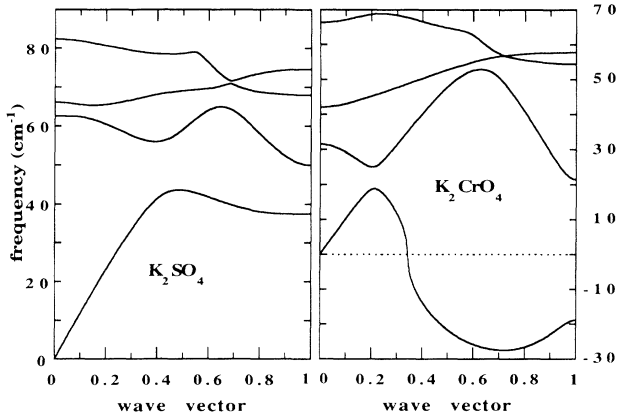

FIG. 3. Four lowest Σ_3-Σ_2 phonon branches in the extended zone scheme for K_2SO_4 and K_2CrO_4 calculated according to the corresponding force models in Table I. In the case of "unstable" imaginary frequencies, their moduli with negative sign are represented.

makes the relative size of potassium ions large enough in this case to stabilize the structure, in a similar form as it happens in selenate compounds when larger alkaline atoms as Rb or Cs are considered [compare the value of $R_T/(R_A+R_X)$ for K_2SO_4 and Cs_2SeO_4 in Table I]. On the other hand, the lowest branch of K_2CrO_4 looks very similar to that of K_2SeO_4, being clearly unstable with a minimum at about $0.7\mathbf{a}^*$. Although the charge distribution inside the tetrahedral groups is quite different, the comparable size of selenate and cromate groups (see Table I) must be the essential factor that determines this strong similarity, not restricted to the lowest Σ_3-Σ_2 phonon branch but also present in the other three branches. The results above suggest that a phase transition of the type observed in potassium selenate is likely to happen in K_2CrO_4 at low temperatures.

In contrast with the oxygen compounds, the calculated branches obtained for K_2ZnCl_4, Rb_2ZnCl_4, and Rb_2ZnBr_4 include in the three cases a rather flat unstable optical branch. This can be related to the experimental fact that in these compounds the BX_4 anions are disordered in the Pnam phase. As shown in Fig. 4, for K_2ZnCl_4, Rb_2ZnCl_4, and in Fig. 5 for Rb_2ZnBr_4, this branch has also a minimum around $0.6-0.7\mathbf{a}^*$, but very weak. A second Σ_3-Σ_2 optical branch is also completely unstable in K_2ZnCl_4, but, in contrast with the results in Refs. 10 and 11 no further unstable branches are obtained. The very different size ratio between the BX_4 anions and the A cations, compared with the one in the oxygen compounds (see Table I), is surely one of the main reasons for the stronger instability of the Zn compounds.

In the cases of Cs_2ZnCl_4 and Cs_2ZnBr_4, which are reported not having phase transition at lower temperatures, the calculated spectra is also unstable, but the imaginary values of the single unstable branch are very close to zero and very sensitive to pressure and stresses. It is reasonable to assume that thermal renormalization effects will be able to stabilize these branches even at very low temperatures. Again, in this case, the larger size of the Cs cations is the main responsible of the stability of the structures compared with the compounds of rubidium. Preliminary results presented in Ref. 14 for Cs_2ZnCl_4 using the same force model differ from those presented here because the calculations in the previous work were done fixing the lattice parameters to the experimental values. The main effect of relaxing lattice parameters consists of a small expansion of the cell. Thus, frequencies obtained in Ref. 14 formally correspond to crystals under a slight external stress, which in the case of Cs_2ZnCl_4 is enough to stabilize the scarcely unstable optical branch. As shown below, a pressure of 5 Kbar is also sufficient to stabilize the whole spectrum of this compound. The differences of the phonon branches calculated with the lattice parameters fixed to the experimental values or with the relaxed values were not significant for the other materials.

The mode polarization vectors at the minimum of the Σ_2 branch (or at the largest imaginary value in the

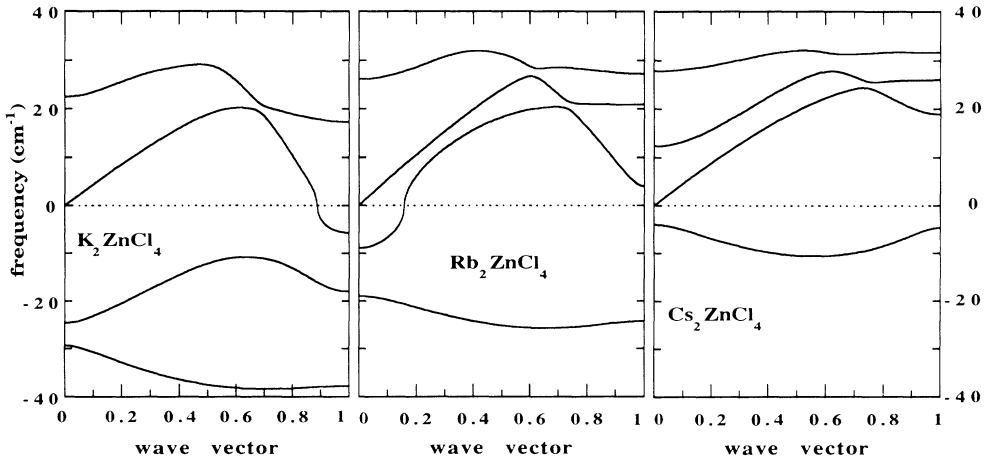

FIG. 4. Four lowest Σ_3-Σ_2 phonon branches in the extended zone scheme for K_2ZnCl_4, Rb_2ZnCl_4, and Cs_2ZnCl_4 calculated according to the corresponding force models in Table I. In the case of "unstable" imaginary frequencies, their moduli with negative sign are represented.

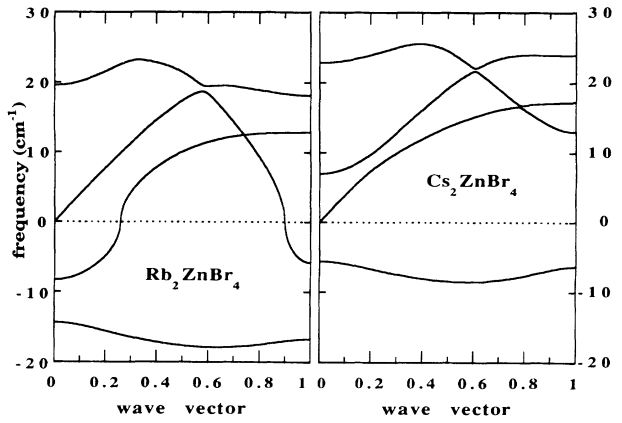

FIG. 5. Four lowest Σ_3-Σ_2 phonon branches in the extended zone scheme for Rb_2ZnBr_4 and Cs_2ZnBr_4 calculated according to the corresponding force models in Table I. In the case of "unstable" imaginary frequencies, their moduli with negative sign are represented.

branch, in the case of the unstable compounds) were calculated for all the A_2BX_4 compounds investigated. In Table II, those corresponding to materials without unstable branches, K_2SO_4, Rb_2SeO_4, and Cs_2SeO_4, are shown. The table lists the values of the nonzero components of $\mathbf{e}(\mu)$ [see Eq. (1)] for the ions and rigid-ionic groups in an asymmetric unit. The vector components for the rest of the atomic units in the unit cell are related to those given in the table by the symmetry properties associated to the irreducible representation Σ_2. It should be noted that the absolute values of the atomic modulation amplitudes have in this case no significance, as an arbitrary normalization of the polarization vectors is used; only their relative values within a given polarization vector are relevant. The obtained polarization vectors for the different materials are very similar especially with respect to the phases. The most significant differences can be observed on the amplitudes of rotations of the tetrahedral ionic groups around the a and b axis.

IV. ENERGY FUNCTION IN THE $\Sigma_2(\frac{1}{3}\mathbf{a}^*)$ SUBSPACE

The existence in some compounds of imaginary frequencies reflects the instability of these systems with respect to some symmetry-breaking distortions of Σ_3-Σ_2 symmetry. The energy minima must correspond to configurations with space groups of lower symmetry than *Pnam;* this latter is then a saddle point of the energy function in the configuration space. As typically the minimum of the most unstable phonon branch (the most negative curvature of the energy function in the configuration space) is situated close to $\frac{2}{3}\mathbf{a}^*(\frac{1}{3}\mathbf{a}^*$ in the reduced zone scheme and symmetry Σ_2) and the lock-in commensurate phase following the IC phase is usually a structure with a tripled cell along the a axis, it is especially interesting to investigate the energy function in the configuration subspace corresponding to distortions of symmetry Σ_2 and wave vector $\frac{1}{3}\mathbf{a}^*$. We have searched the minima of the system energy in this restricted configuration space, i.e., we have determined the distortions of the type given by Eq. (1) that minimize the energy, with the constraints that $\mathbf{q}=\frac{1}{3}\mathbf{a}^*$ and the polarization vector $\mathbf{e}(\mu)$ has symmetry Σ_2.

The polarization vectors obtained for these energy minimizing distortions are listed in Table II. Not surprisingly, they essentially coincided with those calculated for the unstable normal mode at $\mathbf{q}=\frac{1}{3}\mathbf{a}^*$. Consequently, for the "unstable compounds," we have included in Table II only the polarization vectors obtained by the energy minimization procedure. The normalization of the polar-

TABLE II. Displacements (10^4 relative units) and/or rotations (deg), followed by the corresponding phases (in units of 2π), for the asymmetric unit of the *Pnam* structure (chosen as in Ref. 7) describing the predicted polarization vector of either the phonon mode of the lowest Σ_2 branch at $\mathbf{k}=\frac{1}{3}\mathbf{a}^*$ (K_2SO_4, Rb_2SeO_4, Cs_2CeO_4), or, for the rest of the compounds, the Σ_2 distortion with $\mathbf{k}=\frac{1}{3}\mathbf{a}^*$ minimizing the energy, as explained in the text.

		K_2SO_4	Rb_2SeO_4	Cs_2SeO_4	K_2SeO_4	K_2CrO_4
A_α	T_z	79.8,0.094	58.1,0.114	66.2,0.100	120.9,0.114	81.1,0.127
A_β	T_z	103.0,0.316	71.7,0.311	84.2,0.313	149.1,0.321	93.8,0.302
BX_4	T_z	57.8,0.824	38.4,0.804	40.8,0.858	87.9,0.823	57.9,0.787
	R_x	2.86,0.009	3.12,0.016	1.03,−0.012	7.08,0.025	5.34,0.016
	R_y	3.96,0.612	2.82,0.614	2.49,0.601	6.33,0.601	3.60,0.614
		K_2ZnCl_4	Rb_2ZnCl_4	Cs_2ZnCl_4	Rb_2ZnBr_4	Cs_2ZnBr_4
A_α	T_z	291.3,0.185	167.5,0.192	58.0,0.167	177.2,0.137	68.7,0.163
A_β	T_z	260.7,0.300	159.0,0.271	47.0,0.207	173.2,0.263	59.6,0.210
BX_4	T_z	201.4,0.788	149.6,0.742	45.9,0.730	145.8,0.751	57.8,0.722
	R_x	13.87,0.035	10.51,0.023	4.78,0.008	11.24,0.015	5.94,0.008
	R_y	9.48,0.609	4.97,0.625	1.34,0.628	5.23,0.625	1.70,0.626

ization vector has been chosen in this case so that the amplitude of the distortion is one [$|Q|=1$ in (1)] at the energy minimum. The amplitudes listed in Table II represent therefore the actual complex amplitude of the modulation for each independent atom or atomic group at the energy minimum. The phase of the "normal" coordinate Q is also determined in the minimization procedure; in all cases, its value resulted to be $\pi/2$ or its symmetry related ones ($\pi/2+n\pi/3$). They are associated to six equivalent minima corresponding to the three different choices of the first subcell within the tripled cell and to the two equivalent configurations associated to opposite atomic displacements. This particular value obtained for the phase of the mode coordinate Q is especially significant, since a straightforward group-theoretical calculation shows that for this particular phase (or its symmetry related) the energy minimizing distortion transforms the *Pnam* phase into a structure of symmetry $Pna2_1$, which is in fact the symmetry of the tripled lock-in phase observed in all the compounds having the IC phase.

The polarization vectors in Table II for those materials exhibiting an IC phase can be compared with those corresponding to the experimental modulation in the IC phase, which are listed in Table III. The data used in this table has been taken from Refs. 32, 33, 34, and 35, for K_2SeO_4, Rb_2ZnCl_4, Rb_2ZnBr_4, and K_2ZnCl_4 respectively. The atomic modulations for the atoms in the tetrahedral groups have been fitted to rigid-body displacements and rotations. The differences in this table with respect to those published in previous works[7,14] are due to the fact that different sets of experimental data have been used [33,35] and the atomic and ionic modulation amplitudes in Table III correspond to the actual absolute values observed in the experimental IC distortion; i.e., the polarization vectors in Table III correspond to ionic displacements of type (1) with $|Q|=1$ describing the IC distortion. The coincidence of the predicted distortions and those observed is excellent. Typically the phases coincide within a few percent, except for the phase of the translation of one of the cations A, which attains deviations up to 10%. The amplitudes have similar relative values but the discrepancies are somehow larger; see, for instance, the amplitudes of the A ions in K_2ZnCl_4. However, as observed experimentally, the amplitude of the rotation of the tetrahedral groups around the x axis in Rb_2ZnCl_4 and Rb_2ZnBr_4 is approximately twice as large as the one around the y axis, while in K_2ZnCl_4, also in accord with experiment, this ratio decreases to 1.5. For potassium selenate, this ratio significantly decreases, both rotations having comparable amplitudes, but it does not attain the extreme value of 0.6 observed experimentally.

TABLE III. Displacements (10^4 relative units) and/or rotations (deg), followed by the corresponding phases (in units of 2π), for the asymmetric unit of the *Pnam* structure (chosen as in Ref. 7) describing the polarization vector corresponding to the observed Σ_2 static modulation in the IC phase exhibited by some A_2BX_4 compounds. F indicates the degree of fitting of the BX_4 atomic modulations to rigid-body displacements.

		K_2SeO_4	K_2ZnCl_4	Rb_2ZnCl_4	Rb_2ZnBr_4
A_α	T_z	138,0.102	407,0.112	138,0.101	143,0.110
A_β	T_z	184,0.321	391,0.312	160,0.231	147,0.238
BX_4	T_z	116,0.825	237,0.819	122,0.771	118,0.778
	R_x	4.54,0.036	14.10,0.033	10.60,0.024	9.66,0.025
	R_y	7.36,0.643	12.94,0.626	5.10,0.654	4.27,0.654
F		92%	88%	89%	92%

The absolute values of the modulation amplitudes in the theoretical polarization vectors of Table II are also physically significant, as they correspond to the energy minima. It can be seen that Rb_2ZnCl_4 and Rb_2ZnBr_4 have very similar minima and the IC modulation in these two compounds approaches from lower values this predicted minimum. In the case of potassium selenate, on the other hand, the experimental modulation amplitudes in the IC phase are a little larger than those of the predicted energy minimum, except for the rotations of the tetrahedra. Therefore, the energy minimum of the force models are in excellent agreement with the observations, the experimental atomic displacements and group rotations in the IC phase in the four compounds being close to the predicted "saturation" point.

The energy difference (per tripled cell), E_0, between the *Pnam* configuration and the distorted $\Sigma_2(\frac{1}{3}\mathbf{a}^*)$ configuration that minimizes the energy are listed in Table IV for all the "unstable" compounds. The form of the energy function as a function of $|Q|$ (with the orientation of Q in the complex plane fixed along one of the minimizing directions) was also determined. The result for K_2SeO_4 and Rb_2ZnCl_4 is shown in Fig. 6. The form of the curves can be well fitted to a double-well function $a|Q|^2+b|Q|^4$ ($a<0$). It can be seen in Table IV that the deepness of the energy well varies extremely among the different compounds. The wells of the cesium compounds are very shallow, the value of E_Q being one or two orders of magnitude smaller than in the compounds with IC phase transition. The reported stability of the *Pnam* phase up to the low temperatures in the former materials is consistent with this result.

Potassium selenate is an intermediate case, the energy barrier is ten to three times smaller than in the Zn compounds. This is coherent with the much lower transition temperatures and the absence of positional disorder in the *Pnam* phase of potassium selenate. The depth of the energy well in potassium chromate is very small, four times smaller than that of potassium selenate and comparable to that of Cs_2ZnBr_4. This result raises doubt about the possibility of having a structural instability at low temperatures in this compound, in contrast with the conclusion which could be derived from a direct comparison between the strong unstable phonon branch in Fig. 3 for potassium chromate and the one obtained for potassium selenate in Fig. 1.

Similar calculations have been performed for crystals under a pressure of 5 kbar. Pressure effects are introduced by adding to the system energy (in the calculations done with use of WMIN) a term $-p\Delta V$, where p is the pressure and ΔV is the volume change with respect to the

TABLE IV. Energy barrier (E_0) and harmonic coupling between consecutive tripled cells (C) for different applied pressures, calculated as explained in the text [see Eqs. (3) and (4)]. C/E_0 can indicate the character of the transition (displacive or order disorder). T_d and $T_{o\text{-}d}$ are the transition temperatures (K) calculated following Ref. 37 for the displacive and order-disorder cases, respectively. For Cs_2ZnCl_4 and $P=5$ Kbar the *Pnam* structure is not unstable. T_i and T_c are the experimental transition temperatures (if existing) limiting the normal-IC and IC-ferroelectric phases, respectively.

	K_2CrO_4		K_2SeO_4		K_2ZnCl_4		Rb_2ZnCl_4		Cs_2ZnCl_4		Rb_2ZnBr_4		Cs_2ZnBr_4	
Press. (Kbar)	0	5	0	5	0	5	0	5	0	5	0	5	0	5
E_0 (meV)	6.66	3.00	26.61	20.23	347.89	329.45	82.86	71.64	2.60		105.97	84.23	6.01	1.20
C (meV)	7.43	5.16	16.97	15.00	57.67	53.54	25.25	20.71	2.84		28.91	22.24	4.29	1.64
C/E_0	1.12	1.72	0.64	0.74	0.17	0.16	0.30	0.29	1.09		0.27	0.26	0.71	1.37
T_d	33	18	99	81	657	617	204	179	13		257	201	24	7
$T_{o\text{-}d}$	73	51	166	147	565	524	247	203	28		283	218	42	16
T_i			130		553		303				347			
T_c			93		403		192				192			

relaxed structure at zero pressure.[18] The phonon dispersion branches are calculated with the program DYN; pressure effects enter only through the modified mean atomic positions corresponding to the relaxed *Pnam* structure. The main pressure effect in the potential-energy surface is a decrease of the amplitude of the distortion corresponding to the energy minimima, with the structure of the polarization vectors $\mathbf{e}(\mu)$ essentially unchanged, and a smaller depth E_0 of the energy wells (see Table IV). The energy well in the case of Cs_2ZnCl_4 is so low that the application of the mentioned pressure is enough to make it disappear and the structure *Pnam* is stabilized. In accord with this general behavior, the moduli of the imaginary frequencies in the unstable phonon branches decrease in all compounds when pressure is applied. Hence, pressure seems to favor the *Pnam* structure and should in general shift the structural instabilities to lower temperatures. This qualitative general conclusion agrees with the behavior observed in all compounds with respect to the phase transition into the threefold commensurate phase. However, the first structural instability leading to the IC phase has the opposite pressure dependence in K_2ZnCl_4, Rb_2ZnBr_4, and Rb_2ZnCl_4.[36]

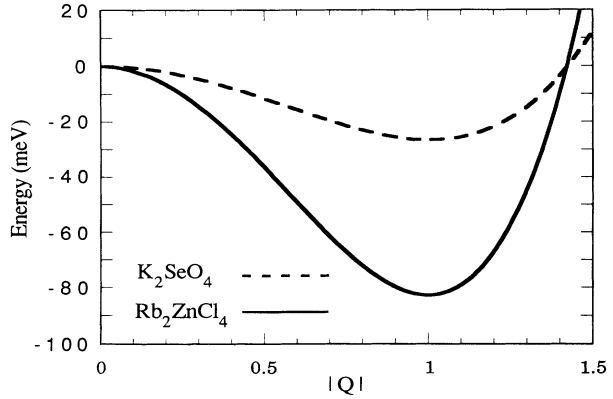

FIG. 6. Lattice energy per tripled cell of Rb_2ZnCl_4 and K_2SeO_4 as a function of the amplitude $|Q|$ of the $\Sigma_2(\frac{1}{3})\mathbf{a}^*$ distortion that minimizes the energy. The curves have been derived using the corresponding force models in Table I. Amplitude units have been chosen in each case so that the energy minimum is at $|Q|=1$.

V. LOCAL-MODE MODEL

Using the preceding energetic calculations, a simplified local-mode model can be developed. We can consider as single local degree of freedom of the system the local value of the amplitude $|Q|$ of the distortion $\Sigma_2\frac{1}{3}\mathbf{a}^*$) that minimizes the energy and was calculated in the preceding section. In the following we will call this local variable x_i, which represents the value of $|Q|$ at the tripled cell i. The variable x includes also a positive or negative sign representing the two equivalent orientations of Q, differing by a phase π in the complex plane. Variations of the mode amplitude along other directions than the a direction are neglected. The energy as a function of an homogeneous $|Q|$ of the distortion $\Sigma_2(\frac{1}{3}\mathbf{a}^*)$ that minimizes the energy and was calculated in the preceding section. In the following we will call this local variable x_i, which represents the value of $|Q|$ at the tripled cell i. The variable x includes also a positive or negative sign representing the two equivalent orientations of Q, differing by a phase π in the complex plane. Variations of the mode amplitude along other directions than the a direction are neglected. The energy as a function of an homogeneous $|Q|$ along the a direction is well described by a double-well function (see Fig. 6). Hence, we can consider as an approximation to the energetics of the critical degrees of freedom of the system, x_i, the following Hamiltonian:

$$H=\tfrac{1}{2}\sum_i m\cdot x_i^2+\sum_i V(x_i)+\tfrac{1}{2}\sum_i C(x_{i+1}-x_i)^2 , \qquad (3)$$

where m is the effective mass of the mode and the local potential $V(x)$ is a double well given by

$$V(x)=E_0(x^2-1)^2 , \qquad (4)$$

where E_0 is the height of the potential barrier and its value for each compound was calculated and listed in the preceding section (see Table IV).

The value of x at the bottom of the wells is ± 1 in the units chosen. The value of C can be derived for each compound by calculating the potential energy per tripled cell of a periodic crystal configuration with the distortion given by the energy minimizing distortion $\Sigma_2(\frac{1}{3}\mathbf{a}^*)$ calculated in the preceding section and listed in Table II, but

with the value of the amplitude Q of the mode being opposite in two consecutive tripled cells ($x_{i+1}=-x_i=-1$). According to (3), this energy is given by E_0+2C. The values of C for each compound calculated in this way are listed in Table IV.

The model Hamiltonian (3) has two important shortcomings. The dimension of the local order parameter is reduced to one, while in fact the amplitude Q of the distorting mode, being a complex number, is two-dimensional. The incommensurate structures corresponding to space-dependent configurations of the phase of the complex order parameter Q are therefore disregarded in this simplified model.

Secondly, the Hamiltonian (3) reduces the system to a one-dimensional problem. For the local mode x, the system is indeed very anisotropic. This was checked by investigating the energy of inhomogeneous configurations of the local mode x along directions perpendicular to the x direction; the values derived for the associated coupling constants were typically one order of magnitude stronger than C. On the other hand, a pure one-dimensional Hamiltonian such as (3) cannot predict a phase transition at finite temperatures. Nevertheless, as shown by Aubry,[37] even in a one-dimensional Hamiltonian of the type (3), a temperature can be found that limits two different thermodynamic regimes with qualitative differences in the degree of order of the average configuration of the system. We can interpret this temperature as a broad estimation of a transition temperature between the normal *Pnam* phase and the tripled ferroelectric phase, disregarding any intermediate IC phase, which is excluded from the model. The value of this "transition" temperature has been derived in Ref. 37 in the limits $C \ll E_0$ ("order-disorder case") and $C \gg E_0$ ("displacive case"), being approximately $0.844C/k_B$ and $0.4\sqrt{(CE_0)}$, respectively. In Table IV, the ratio C/E_0 for each compound is given together with the transition temperatures $(T_{o\text{-}d}, T_d)$ for the two limits, calculated according to the expressions above. For comparison, the experimental transition temperatures T_i, T_c (if existing) corresponding to the normal-IC and IC-ferroelectric phase transitions, respectively, are also listed. The values of C/E_0 for K_2ZnCl_4, Rb_2ZnBr_4, and Rb_2ZnCl_4 are rather small, increasing in this order from one compound to another and being in the three cases within the range of the order-disorder case.[33] Therefore, for them, the transition temperature $T_{o\text{-}d}$ should be taken as the relevant theoretical one. In the other materials the values of C/E_0 fall in an intermediate range between both regimes. Accordingly, the two temperatures T_d and $T_{o\text{-}d}$ can be taken as limits for a qualitative interpolation between both cases. Comparing experimental and theoretical transition temperatures, it is clear that despite the rough simplifications of the model, the theoretical values achieve in general a correct estimation of the temperature range where the structural instabilities are actually taking place. According to the model, a phase transition can be expected in potassium chromate in the range 30–70 K.

In order to characterize pressure effects, a similar parallel calculation was performed for a pressure of 5 Kbar. The results are also listed in Table IV. In all cases, the theoretical transition temperatures decrease, in accord with the experimental behavior of T_c.[36] The peculiar opposite behavior for the normal-IC transition temperature T_i observed in the Zn compounds cannot be explained, as the model disregards the IC phase. However, the pressure dependence of the model parameters in potassium selenate (and also in potassium chromate) differs significantly from the one obtained for the Zn compounds, in the sense that C/E_0 increases with pressure in potassium selenate, while the opposite happens in the case of the Zn compounds. This significant difference distinguishes against the two groups which exhibit a very different phonon dynamics in the simulations.

VI. CONCLUSIONS

The present study and the results in Refs. 7 and 14 indicate that a simple empirical rigid-ion force model only fitted to static structural data is enough for explaining the eventual presence of an incommensurate instability at lower temperatures in the A_2BX_4 compounds. For all the materials exhibiting the *Pnam*-IC phase transition, an unstable Σ_2 phonon branch with a minimum close to $\frac{1}{3}\mathbf{a}^*$ is obtained. The calculated polarization vector of the soft or unstable mode, which should determine the structure of the IC modulation, is rather insensitive to the details of the interatomic forces. For each compound having an IC phase, the calculated polarization vector is in excellent agreement with the experimental one determined from structural data of the IC phase.

The experimental evidence that in the Zn compounds, in contrast with potassium selenate, the BX_4 tetrahedra are somehow disordered in the normal phase and a soft-mode mechanism is not present, can be correlated with the presence in the lattice-dynamics simulations of these compounds of a rather flat completely unstable phonon branch. On the other hand, those compounds with no reported normal-IC phase transition are "well behaved" in the simulations, the calculated phonon branches being essentially stable. Only in the case of K_2CrO_4, the simulations indicate that an incommensurate structural instability at very low temperatures may exist. It is also important that the results for Rb_2SeO_4 indicate an incomplete softening of the lowest Σ_2 phonon branch.

The actual presence of an incommensurate instability depends basically on the effective volume of the A cations. The empirical relation of the effective atomic sizes with the basic types of commensurate structures observed in the A_2BX_4 family has been thoroughly discussed in Refs. 38–40. The present study indicates that the ultimate cause of the incommensurate instability is also a simple volume effect, as suggested in Refs. 41 and 7. Indeed, as shown in Fig. 7, the experimental normal-IC transition temperature is roughly correlated with the ratio between the A ionic radius and the sum of the ionic radius of X and B. The existence of an IC phase is limited to a small range of values for this size ratio (0.57–0.85), and the normal-IC transition temperature steadily increases as the size ratio decreases. It is

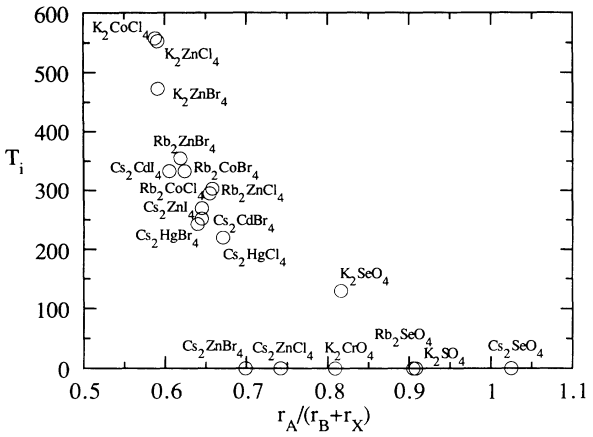

FIG. 7. Transition temperature T_i limiting the *Pnam* and IC phases for a set of A_2BX_4 compounds as a function of the ratio $r_A/(r_B+r_X)$, where r_i are the ionic radii. In most cases, the average experimental value for the distance B-X in the BX_4 tetrahedral groups (RT), if known, has been taken as r_B+r_X. For comparison, those compounds having no phase transition have been indicated in the diagram as a point with $T_i=0$.

significant that in this diagram the abscissa values associated to potassium chromate and potassium selenate are very close, explaining the similarities of their lattice-dynamics results. The fact that Cs_2ZnCl_4 and Cs_2ZnBr_4 are reported to have no phase transition leaves K_2SeO_4 in Fig. 7 as an isolated case somehow disconnected from the general trend. This different behavior is probably related to the very different charge distribution inside the anionic groups (see Table I). A simple linear fitting of the experimental transition temperatures T_i in terms of Q_B and $RT/(R_A+R_X)$ (see Table I) has been done using the following expression:

$$T_{\text{fit}}=\alpha+\beta[RT/(R_A+R_X)]+\gamma Q_B \ . \tag{5}$$

The results of the fit are shown in Table V. The four experimental values of T_i can be well reproduced and the adjusted expression predicts the stability or instability of some of the other compounds in qualitative accord with the energetic and dynamic models reported in the preceding sections. In broad terms, it can be said that a larger value of Q_B tends to unstabilize the *Pnam* structure. On the other hand, larger A-X distances, or larger sizes of the cations A, in comparison with the size of the anionic groups tend to stabilize the *Pnam* normal phase.

TABLE V. Experimental normal-IC transition temperature (T_i) and calculated transition transition temperature (T_{fit}) using expression (5) with $\alpha=-4664.65$ K, $\beta=8438.00$ K, and $\gamma=815.93$ K e^{-1}.

A_2BX_4	T_i	T_{fit}
K_2CrO_4		4
K_2SO_4		−154
K_2SeO_4	130	131
Rb_2SeO_4		−7
Cs_2SeO_4		−111
K_2ZnCl_4	553	552
Rb_2ZnCl_4	303	304
Cs_2ZnCl_4		−25
Rb_2ZnBr_4	347	347
Cs_2ZnBr_4		29

The peculiar pressure dependence of the IC transition temperature exhibited by the Zn compounds could not be properly reproduced by the models discussed in the present work. Probably, the parametrization for each compound of a more complex model where the two-dimensional character of the local order parameter is taken into account can be enough to understand this effect.

An important feature of all the simulations is that the unstable or soft-mode branch is always an optical branch in the extended zone scheme or the result of an anticrossing of an optical branch with the Σ_3-Σ_2 acoustic branch. Hence, microscopic models, where a single local mode is considered and the corresponding phonon branch is fitted to the experimental acoustic branch, as proposed by Iizumi *et al.*,[2] are inconsistent with the basic mechanism of the transition. They disregard the important fact that the part of the acoustic phonon branch, where the softening takes place (see Figs. 1 and 3) is indeed the continuation of an optical branch. In this context models with two local modes giving place to two phonon branches, as proposed in Ref. 42, are more likely to simulate the mechanism of the transition.

ACKNOWLEDGMENTS

We gratefully acknowledge the help and support of Alberto Criado (University of Sevilla), who provided the program DYN. This work was partially supported by the Universidad del Pais Vasco (Project UPV 063.310-E180/90).

[1]K. Itoh, A. Hinasada, H. Matsunaga, and E. Nakamura, J. Phys. Soc. Jpn. **52**, 664 (1983).
[2]M. Iizumi, J. D. Axe, G. Shirane, and K. Shimaoka, Phys. Rev. B **15**, 4392 (1977).
[3]A. Kalman, J. S. Stephens, and D. W. J. Cruickshank, Acta Crystallogr. Sec. B **26**, 1451 (1970).
[4]N. Yamada and T. Ikeda, J. Phys. Soc. Jpn. **53**, 2555 (1984).
[5]J. D. Axe, M. Iizumi, and G. Shirane, in *Incommensurate Phases in Dielectrics. Part II, Materials,* edited by R. Blinc and A. P. Levanyuk (North-Holland, Amsterdam, 1986), p. 1.
[6]H. Z. Cummins, Phys. Rep. **185**, 211 (1990).
[7]I. Etxebarria, J. M. Perez-Mato, and A. Criado, Phys. Rev. B **42**, 8482 (1990).
[8]J. M. Perez-Mato, F. J. Zúñiga, and G. Madariaga, Phase Transitions **16/17**, 439 (1989).
[9]M. Haque and J. R. Hardy, Phys. Rev. B **21**, 245 (1980).
[10]V. Katkanant, P. J. Edwarson, J. R. Hardy, and L. Boyer, Phase Transitions **15**, 103 (1989).

[11]P. J. Edwarson, V. Katkanant, J. R. Hardy, and L. Boyer, Phys. Rev. B **15**, 8470 (1987).
[12]V. Katkanant, P. J. Edwarson, J. R. Hardy, and L. Boyer, Phys. Rev. Lett. **57**, 2033 (1986).
[13]H. M. Lu and J. R. Hardy, Phys. Rev. B **42**, 8339 (1990).
[14]J. M. Perez-Mato, I. Etxebarria, and G. Madariaga, in Proceedings of the 11th General Conference of the Condensed Matter Division of the EPS [Phys. Scr. T **39**, 81 (1991).
[15]S. L. Chaplot and K. R. Rao, Phys. Rev. B **33**, 4327 (1986).
[16]S. L. Chaplot and K. R. Rao, J. Phys. C **16**, 3045 (1983).
[17]J. A. Nelder and R. Mead, Comput. J. **7**, 308 (1965).
[18]W. R. Busing, Acta Crystallogr. Sec. A **28**, S252 (1972).
[19]J. A. McGinnety, Acta Crystallogr. Sec. B **28**, 2845 (1972).
[20]I. Takahashi, A. Onodera, and Y. Shiozaki, Acta Crystallogr. Sec. C **43**, 179 (1987).
[21]F. J. Zúñiga, T. Breczewski, and A. Arnaiz, Acta Crystallogr. Sec. C **47**, 638 (1991).
[22]J. A. McGinnety, Inorg. Chem. **13**, 1057 (1974).
[23]B. Morosin and E. C. Lingafelter, Acta Crystallogr. **12**, 744 (1959).
[24]M. Quilichini, P. Bernede, J. Lefebvre, and P. Schweiss, J. Phys. Condens. Matter **2**, 4543 (1990).
[25]S. Secco and J. Trotter, Acta Crystallogr. Sec. C **39**, 317 (1983).
[26]J. C. de Pater, Acta Crystallogr. Sec. B **35**, 299 (1979).
[27]D. Liu, H. M. Lu, F. G. Ullman, and J. R. Hardy, Phys. Rev. B **43**, 6202 (1991).
[28]M. Quilichini and J. Pannetier, Acta Crystallogr. Sec. B **39**, 657 (1983).
[29]J. A. McGinnety, J. Am. Chem. Soc. **94**, 8406 (1972).
[30]A. Criado, A. Conde, and R. Marquez, Acta Crystallogr. Sec. A **40**, 696 (1984).
[31]I. Etxebarria, M. Lynden-Bell, and J. M. Perez-Mato (unpublished).
[32]J. M. Perez-Mato, G. Madariaga, and F. J. Zúñiga, Phase Transitions **16/17**, 445 (1989).
[33]A. Hedoux, D. Grebille, J. Jaud, and G. Godefroy, Acta Crystallogr. Sec. B **45**, 370 (1989).
[34]A. C. R. Hogervorst and R. B Helmholdt, Acta Crystallogr. Sec. B **44**, 120 (1988).
[35]M. Quilichini, P. Bernede, J. Lefebvre, and P. Schweiss, J. Phys. Condens. Matter **2**, 4543 (1990).
[36]K. Gesi, Ferroelectrics **64**, 97 (1985).
[37]S. Aubry, J. Chem. Phys. **62**, 3217 (1975).
[38]B. V. Beznosikov and K. S. Aleksandrov, Kristallografiya **30**, 509 (1985) [Sov. Phys. Crystallogr. **30**, 295 (1985)].
[39]B. V. Beznosikov and K. S. Aleksandrov, Kristallografiya **30**, 919 (1985) [Sov. Phys. Crystallogr. **30**, 533 (1985)].
[40]B. V. Beznosikov and K. S. Aleksandrov, Kristallografiya **30**, 923 (1985) [Sov. Phys. Crystallogr. **30**, 535 (1985)].
[41]H. Nakayama, N. Nakamura, and H. Chihara, Bull. Chem. Soc. Jpn. **60**, 99 (1987).
[42]Z. Y. Chen and M. B. Walker, Phys. Rev. Lett. **65**, 1223 (1990).